

Multipass relativistic high-order-harmonic generation for intense attosecond pulsesMatthew R. Edwards^{1,*} and Julia M. Mikhailova^{1,2,†}¹*Department of Mechanical and Aerospace Engineering, Princeton University, Princeton, New Jersey 08544, USA*²*Prokhorov General Physics Institute, Russian Academy of Sciences, 119991, Moscow, Russia*

(Received 8 September 2015; published 24 February 2016)

We demonstrate that the total reflected field produced by the interaction of a moderately relativistic laser with dense plasma is itself an efficient driver of high-order-harmonic generation. A system of two or more successive interactions of an incident laser beam on solid targets may therefore be an experimentally realizable method of optimizing conversion of laser energy to high-order harmonics. Particle-in-cell simulations suggest that attosecond pulse intensity may be increased by up to four orders of magnitude in a multipass system, with decreased duration of the attosecond pulse train. We discuss high-order-harmonic wave-form engineering for enhanced attosecond pulse generation with an electron trajectory model, present the behavior of multipass systems over a range of parameters, and offer possible routes towards experimental implementation of a two-pass system.

DOI: [10.1103/PhysRevA.93.023836](https://doi.org/10.1103/PhysRevA.93.023836)**I. INTRODUCTION**

Relativistic high-order-harmonic generation (HHG) on solid-density targets offers a path towards the creation of intense attosecond pulses [1,2]. The intensity limit of current laser technology provides substantial motivation for maximizing the intensity of generated attosecond pulses at fixed driving laser power [3]. Experimental, computational, and theoretical work has explored relativistic HHG [4–13], though attention has been focused almost entirely on single-frequency driving lasers. Some previous studies [14–17] have suggested that two-color beams can produce relativistic harmonics more effectively than single-frequency wave forms. Analogous work on two-color beams [18,19] and wave-form optimization [20–22] has been conducted for gas-phase HHG, where multicolor beams have been shown to improve attosecond pulse characteristics. The short durations, and resulting wide spectra, of the laser pulses interesting for relativistic HHG make the addition of more than two or three harmonics difficult. In this paper we show that the wave form created by relativistic HHG is under many conditions itself an excellent choice for driving further harmonic generation and that a system comprising two or more passes of a relativistic laser on solid targets provides remarkable gains in attosecond pulse intensity. Recently published work [23] has found multipass enhancement in the case of normal incidence in one dimension. Here we provide a comprehensive description of multipass systems, covering oblique incidence, finite plasma-density gradients, and two-dimensional effects.

Electron trajectory analysis of HHG associates high attosecond pulse intensities with increased electron velocity and acceleration at the time of emission, parallel and perpendicular to the reflected wave vector, respectively [12,14]. Examination of the trajectories followed by emitting electrons (Fig. 1) suggests that ideal wave forms create a large transverse (y -direction) electron velocity between times t_1 and t_2 , where most of the electron energy is acquired. Between t_2 and t_3 ,

the electrons are turned by the laser magnetic field and slowed in y by the laser electric field. The net effect of the ion field varies with parameters; in Fig. 1 the ion static field adds no net energy between t_2 and t_3 , since the z positions at t_2 and t_3 are equidistant from the ion sheet. Optimized attosecond pulse emission requires minimizing the loss of energy between t_2 and t_3 and maximizing the field at t_3 , which suggests a large field gradient between t_2 and t_3 . Addition of a second harmonic field can increase the field gradient [14], but a sharp field gradient is also characteristic of the total reflected field for relativistic high-order-harmonic generation.

II. METHODS

We conducted particle-in-cell (PIC) simulations to study the cumulative effect of successive relativistic laser-plasma surface interactions, using a modified version of the one-dimensional (1D), three-velocity PIC code BOPS [24] and the two-dimensional (2D) implementation of the code EPOCH [25]. All 1D simulations were performed with $\Delta x/\lambda = \Delta t/T_L = 0.0012$ at $\lambda = 800$ nm and 150 particles per cell, where Δx is the cell size and Δt is the time step. The spatial resolution of the 2D simulations was $\Delta x/\lambda = 0.004$. Due to the high laser intensities involved, we consider a fully ionized plasma, and both ions and electrons are mobile. Solid targets produce overdense plasma ($N = n_e/n_c > 1$, where n_e is the electron number density and $n_c = m_e \omega_L^2 / 4\pi e^2$ is the plasma critical density), and here we study P -polarized relativistic driving lasers ($a_0 = E_0/E_{\text{rel}} > 1$, where $E_{\text{rel}} = m_e \omega_L c / e$). The plasma is initially at zero temperature and is sufficiently thick (1λ) to be treated as semi-infinite for the pulse lengths ($\tau = 5$ fs FWHM, intensity) used for these results (where not otherwise noted).

III. RESULTS

We initially consider a two-pass mechanism in which the reflected light from the first interaction maintains its intensity until the second interaction; i.e., the reflected field of the first simulation is exactly the incident field of the second simulation. Figure 2(a) illustrates the spectral enhancement provided by the second interaction over a single reflection.

*mredward@princeton.edu

†j.mikhailova@princeton.edu

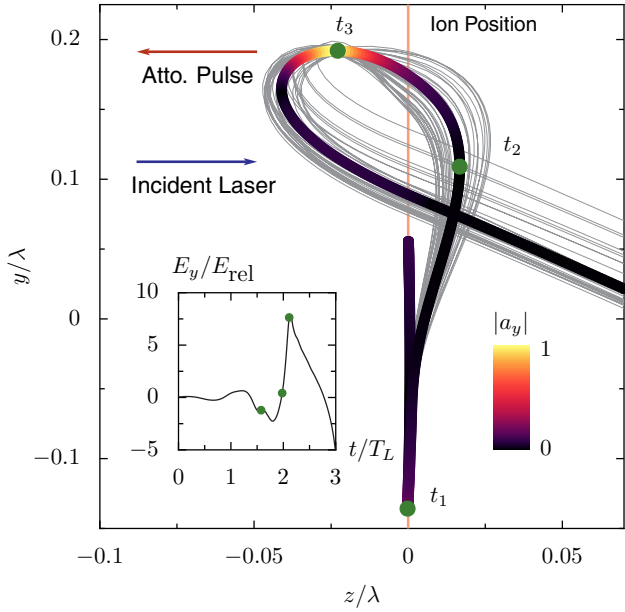


FIG. 1. Trajectories followed by electrons during attosecond pulse generation on thin foil target (thickness $\lambda/200$), at normal incidence with $N = 500$ and $a_0 = 10$. The color of the mean trajectory corresponds to the absolute value of the transverse acceleration, normalized by its maximum value. The initial electron position is $(0,0)$. Inset: Electric field experienced by emitting electron bunch, with fields values at times t_1 , t_2 and t_3 marked with green circles.

The inset shows the filtered high frequency (attosecond pulse) intensity, confirming that the second interaction maintains the phase coherence of the first and demonstrating both improved pulse isolation and a two-order-of-magnitude increase in intensity.

The enhancement of attosecond pulse intensity as a result of the second interaction varies with plasma density and laser intensity. Figure 2(b) shows the ratio of the second-pass attosecond pulse intensity (I_2) to the pulse intensity after the first pass (I_1) for different a_0 and N . The attosecond pulses are calculated by filtering the reflected spectrum to include only $\omega/\omega_L > 10$. For fixed N there is a particular value of a_0 at which the maximum enhancement obtained in the second pass occurs; at higher densities this corresponds to higher a_0 . Additional spectra, corresponding to the highest two-pass gain values of a_0 for $N = 100$ and $N = 200$, are presented in Figs. 2(c) and 2(d).

Though a two-pass system is most readily realized, additional successive passes may continue to increase high-order-harmonic conversion efficiency for values of a_0/N below the two-pass optimum. Figure 3(a) illustrates that the maximum pulse amplification sometimes occurs only after multiple passes through the system. For these results the reflected field of each simulation is supplied as the incident field of the next, so that energy losses in the plasma are accounted for, but energy losses due to refocusing onto the target are not. Lower incident intensities require multiple passes before HHG is significantly enhanced, but the ultimate gains can be large, with 11 passes at $a_0 = 5$ producing a brighter attosecond pulse than a single interaction at $a_0 = 30$. Figure 3(b) shows the field steepening that occurs for alternate changes in fields

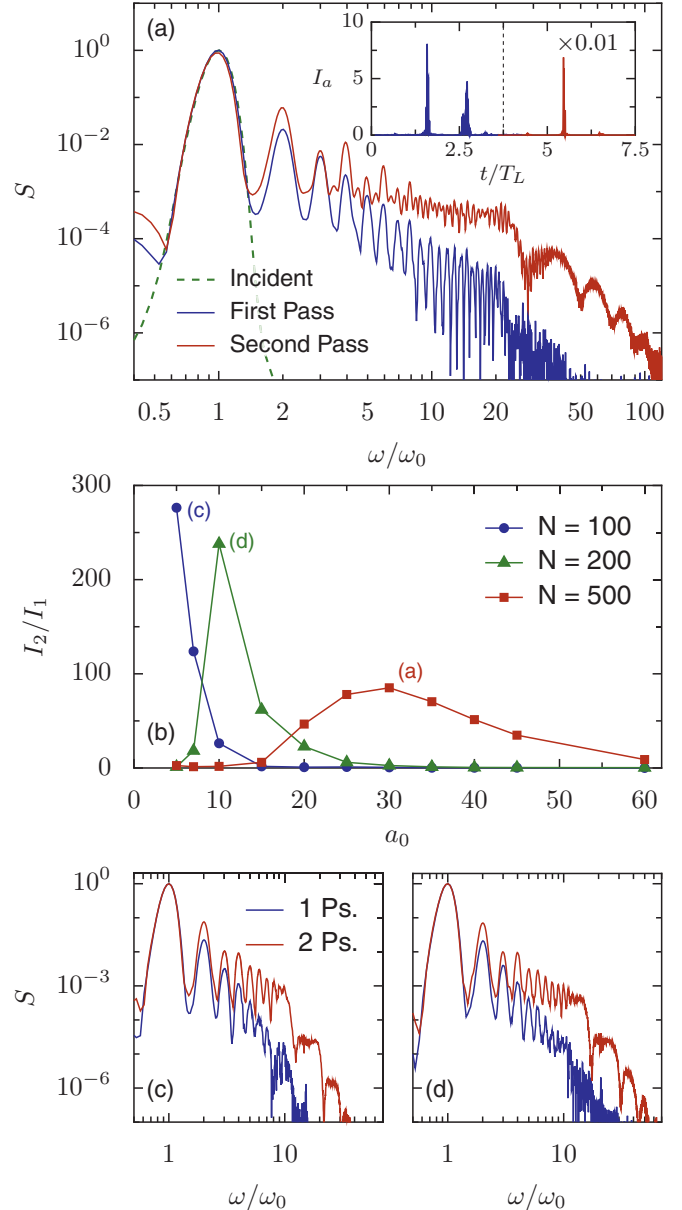


FIG. 2. Enhancement of HHG through two-pass interaction. (a) The spectra of the incident (green dashed line), first-pass reflected (blue, lower solid line), and second-pass reflected (red, upper solid line) fields, showing a substantial increase in HHG efficiency at $a_0 = 30$, $N = 500$, and $\theta_L = 30^\circ$ (angle of incidence) on a flat plasma surface. Inset: Corresponding attosecond pulses ($10 < \omega/\omega_L$) generated after first pass (left) and second pass (right). (b) The attosecond pulse intensity after two passes (I_2) compared to intensity after a single pass (I_1) for varied a_0 and N . $\theta_L = 30^\circ$, $10 < \omega/\omega_L$. (c) The reflected spectra after one (blue, lower line) and two (red, upper line) passes at $a_0 = 5$ and $N = 100$ and (d) $a_0 = 10$ and $N = 200$.

sign after each pass. The produced wave form is reminiscent of that found to be optimal for two-color driving beams [14]. After multiple passes, or at high initial laser intensity, harmonic generation is so efficient that the resulting wave form loses its suitability for driving additional harmonics. This saturation is characterized by the division of high-frequency energy among multiple attosecond pulses per optical cycle, resulting in the

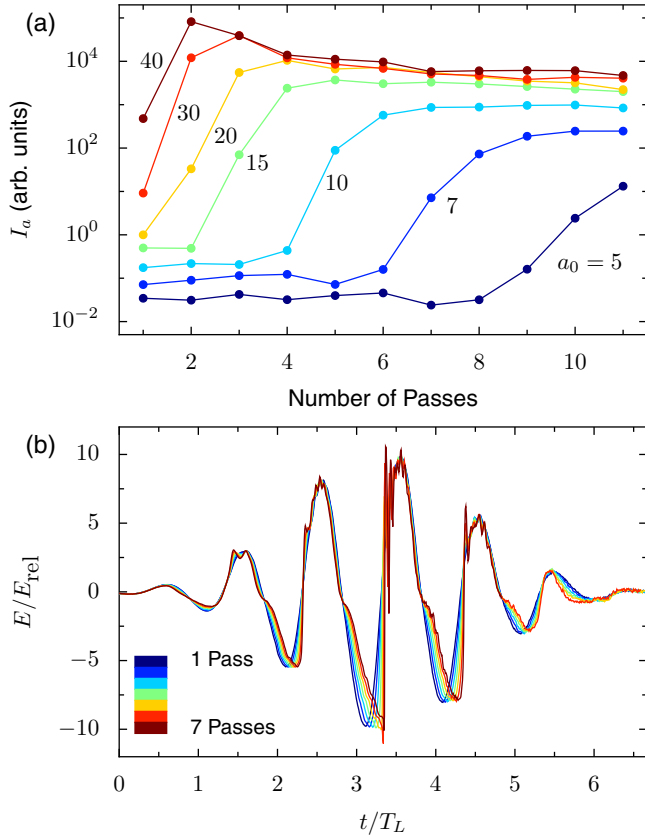


FIG. 3. Effect of multiple interactions on attosecond pulse intensity and electric field shape. (a) Attosecond pulse intensity for each pass through a multipass configuration, demonstrating the effect of a_0 on the optimum number of passes on a flat surface at $\theta_L = 30^\circ$, $N = 500$, $\tau = 5$ fs (FWHM), and harmonics filtered by $30 < \omega/\omega_L < 100$. (b) Change in shape of electric field after each pass for the data at $a_0 = 10$.

loss of phase coherence and the disruption of emitting electron trajectories.

The advantages of a multipass system are reduced for surfaces with finite exponential plasma density gradients [$n_e(x) \propto \exp(x/L)$ where $L/\lambda \approx 0.05-0.1$], partially because density gradients at the plasma surface already substantially increase HHG efficiency [2,13], and partially due to additional energy loss in the plasma as a result of a finite gradient. Previous work on two-color beams [14] has shown that for a finite gradient gains in attosecond pulse intensity from wave shaping are reduced to about an order of magnitude. For longer ($\tau = 30$ fs) pulses [Fig. 4(a)], an interaction with a flat surface before a second interaction with a finite gradient produces attosecond pulses up to 10–30 times brighter than a single interaction with a finite gradient at the same conditions, with a dependence on N and a_0 which appears similar to, though less well defined than, the infinitely steep density-gradient case. When the first interaction surface also has a finite gradient [Fig. 4(b)], the additional loss of energy in the the first plasma gradient reduces intensity gains, though the enhancement can still be substantial. This case may also be advantageous for longer duration incident pulses ($\tau \gtrsim 20$ fs), since the interaction of longer pulses with multiple finite gradients can

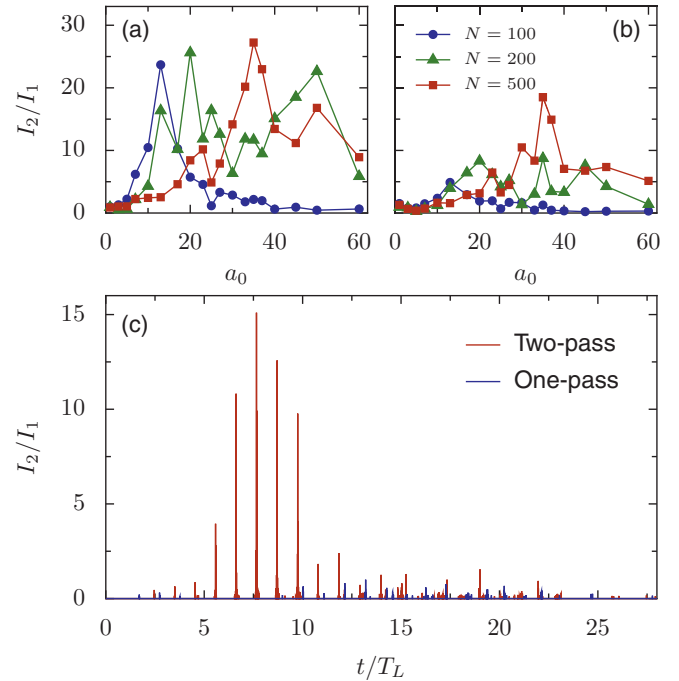


FIG. 4. Multipass configuration with a finite plasma density gradient. (a) Attosecond pulse intensity after second pass on finite gradient ($L/\lambda = 0.05$) where the first pass is either (a) on an infinite plasma density gradient or (b) on the same density gradient as the second pass. For both cases, the first-pass intensity used for normalization, I_1 , is calculated for a single pass on a finite gradient. (c) Comparison of attosecond pulse trains generated at $N = 200$, $a_0 = 40$, $L/\lambda = 0.05$, and $\tau = 30$ fs with (red) and without (blue) an initial pass on a flat plasma surface at the same intensity and maximum density. The intensity of the largest single-pass attosecond pulse is 1. For all results, $\theta_L = 30^\circ$ and $30 < \omega/\omega_L < 100$.

produce dramatic shortening of the attosecond pulse train in addition to intensity gains [Fig. 4(c)].

To check the validity of reducing the above analysis to one dimension, 2D simulations were performed for both one- and two-pass configurations. In Fig. 5(a), an incident beam which reaches $a_0 = 20$ is focused between two plasma surfaces ($N = 200$), producing substantially enhanced harmonics compared to both the intermediate field between the two plasma surfaces and the evolved single-pass field in Fig. 5(b). Figure 6(a) indicates that the second interaction does not result in increasing divergence for the second beam; the smaller generation area is offset by the shorter wavelength of the generated light. The inset spectrum exhibits the same characteristics as the 1D spectra in Fig. 2. Figure 6(b) shows how the beam widths of the different frequencies contained in the incident and reflected fields evolve throughout the interaction, demonstrating both that a small beam diameter can be maintained through both passes and that the two-pass high-order harmonics retain a relatively small divergence. The agreement between 1D and 2D simulations suggests that the spatial distribution of harmonics and beam focusing do not substantially reduce multipass efficiency.

Experimental realization of a two-pass configuration is possible either by placing the two interaction surfaces so

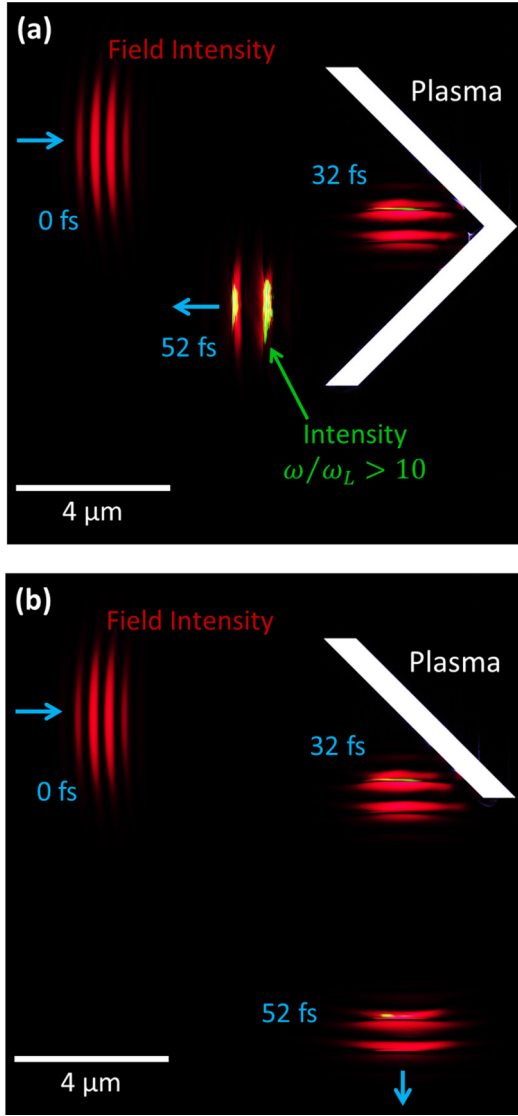


FIG. 5. 2D simulations comparing two-pass (a) and one-pass (b) interactions. An incident laser (red, $a_0 = 20$, $\tau = 5$ fs) interacts with two (a) or one (b) plasma surfaces (white, $N = 200$), showing substantially enhanced high-order harmonics (green) in the two-pass case. Note that in these images the colors corresponding to the attosecond pulse intensities are saturated for visibility, so the pulses appear spatially larger than their true extent.

close together that both are within the Rayleigh length of the driving laser [Fig. 7(a)] or by refocusing the reflected pulse with a focusing mirror onto a new surface [Fig. 7(b)]. Advances in additive manufacturing may allow geometries such as that shown in Fig. 7(a) to be fabricated practically [26]. A configuration of multiple reflections at finite angle of incidence ($\theta_L \neq 0$) between two parallel surfaces may not be viable, because the sign of the angle of incidence determines which of the two attosecond pulses that would appear during each optical cycle at normal incidence is enhanced. In a parallel-plate configuration at oblique incidence, θ_L changes sign with each reflection, so that any high-order harmonics in the incident beam will be half a cycle out of phase at the second reflection and will suppress rather than enhance

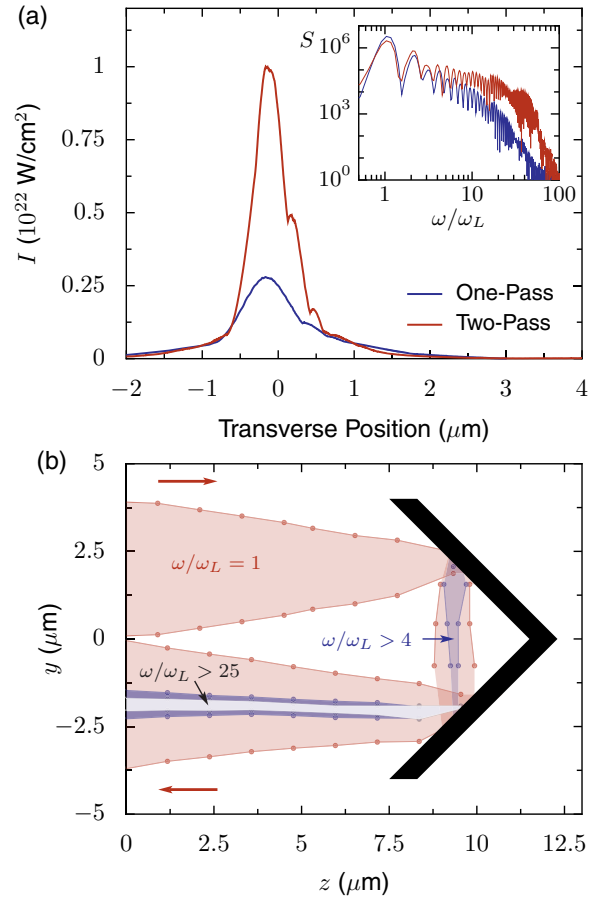


FIG. 6. (a) The transverse distribution of reflected intensity from 2D simulations (same as Fig. 5), showing spatial narrowing, after one pass (blue, lower line) and two passes (red, upper line). Inset: spectra of reflected fields in both cases (red, upper line is two-pass spectrum), demonstrating quantitatively similar behavior to 1D simulations. (b) Spatial FWHM of fundamental (red), moderate harmonics $4 < \omega/\omega_L < 20$ (blue) and high harmonics $25 < \omega/\omega_L < 40$ (gray) for focused two-pass interaction.

the creation of new attosecond pulses. This effect is directly related to the suppression of attosecond pulses by second-order harmonic light for particular values of the relative phase [14]. A geometry which maintains the sign of the angle of incidence is therefore required. The behavior of multipass configurations at different angles of incidence is qualitatively similar, with

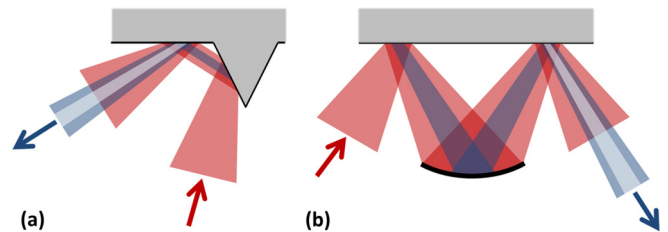


FIG. 7. Experimental multipass configurations. Multiple interactions may be realized by (a) focusing the driving beam such that two surfaces are within the Rayleigh length or (b) refocusing the reflected harmonics onto a second surface.

some variation in the magnitude of enhancement depending on the efficiency of underlying one-pass configuration. Though refocusing [Fig. 7(b)] will result in the loss of very high-order harmonics from the first pass due to the difficulty of reflecting extreme ultraviolet and x-ray light, the enhanced efficiency of the second-pass generation is driven primarily by the lower order harmonics; the high-order harmonics are too weak and high in frequency to have a significant effect on electron motion.

IV. CONCLUSION

In comparison to two-color driving beams, multipass HHG is advantageous for creating intense attosecond pulses because the different frequencies are automatically formed with the same polarization and an appropriate phase difference. Multipass HHG offers a realizable method for approaching the optimal efficiency of HHG in the short-pulse regime, where

few tools for wave-form engineering are effective. In this paper we have provided computations on multipass configurations for experimentally relevant parameters, including the effects of oblique incidence, finite plasma gradients, and two dimensions, and suggested possible routes towards experimental implementation.

ACKNOWLEDGMENTS

This work is partially supported by the NSF under Grant No. PHY 1506372. M.R.E. gratefully acknowledges the support of the NSF through a graduate research fellowship. We would like to thank Paul Gibbon for help with the BOPS code. This work was performed at the High Performance Computing Center at Princeton University. The development of the EPOCH code was funded in part by UK EPSRC Grants No. EP/G054940/1, No. EP/G056803/1, No. EP/G055165/1, and No. EP/M022463/1.

-
- [1] F. Krausz and M. Ivanov, *Rev. Mod. Phys.* **81**, 163 (2009).
 - [2] C. Thaury and F. Quéré, *J. Phys. B* **43**, 213001 (2010).
 - [3] P. Gibbon and E. Forster, *Plasma Phys. Controlled Fusion* **38**, 769 (1996).
 - [4] P. Gibbon, *Phys. Rev. Lett.* **76**, 50 (1996).
 - [5] Yu. M. Mikhailova, V. T. Platonenko, and S. Rykovanov, *JETP Lett.* **81**, 571 (2005).
 - [6] B. Dromey, M. Zepf, A. Gopal, K. Lancaster, M. Wei, K. Krushelnick, M. Tatarakis, N. Vakakis, S. Moustazis, R. Kodama, M. Tampo, C. Stoeckl, R. Clarke, H. Habara, D. Neely, S. Karsch, and P. Norreys, *Nat. Phys.* **2**, 456 (2006).
 - [7] F. Quéré, C. Thaury, P. Monot, S. Dobosz, P. Martin, J.-P. Geindre, and P. Audebert, *Phys. Rev. Lett.* **96**, 125004 (2006).
 - [8] T. Baeva, S. Gordienko, and A. Pukhov, *Phys. Rev. E* **74**, 065401 (2006).
 - [9] T. J. M. Boyd and R. Ondarza-Rovira, *Phys. Rev. Lett.* **101**, 125004 (2008).
 - [10] A. A. Gonoskov, A. V. Korzhimanov, A. V. Kim, M. Marklund, and A. M. Sergeev, *Phys. Rev. E* **84**, 046403 (2011).
 - [11] P. Heissler, R. Hörlein, J. M. Mikhailova, L. Waldecker, P. Tzallas, A. Buck, K. Schmid, C. M. S. Sears, F. Krausz, L. Veisz, M. Zepf, and G. D. Tsakiris, *Phys. Rev. Lett.* **108**, 235003 (2012).
 - [12] J. M. Mikhailova, M. V. Fedorov, N. Karpowicz, P. Gibbon, V. T. Platonenko, A. M. Zheltikov, and F. Krausz, *Phys. Rev. Lett.* **109**, 245005 (2012).
 - [13] F. Dollar, P. Cummings, V. Chvykov, L. Willingale, M. Vargas, V. Yanovsky, C. Zwick, A. Maksimchuk, A. G. R. Thomas, and K. Krushelnick, *Phys. Rev. Lett.* **110**, 175002 (2013).
 - [14] M. R. Edwards, V. T. Platonenko, and J. M. Mikhailova, *Opt. Lett.* **39**, 6823 (2014).
 - [15] S. Mirzanejad and M. Salehi, *Phys. Rev. A* **87**, 063815 (2013).
 - [16] A. Tarasevitch, R. Kohn, and D. Von Der Linde, *J. Phys. B* **42**, 134006 (2009).
 - [17] A. Tarasevitch and D. von der Linde, *Eur. Phys. J. Special Topics* **175**, 35 (2009).
 - [18] J. Mauritsson, P. Johnsson, E. Gustafsson, A. L’Huillier, K. J. Schafer, and M. B. Gaarde, *Phys. Rev. Lett.* **97**, 013001 (2006).
 - [19] T. Pfeifer, L. Gallmann, M. J. Abel, D. M. Neumark, and S. R. Leone, *Opt. Lett.* **31**, 975 (2006).
 - [20] S. B. P. Radnor, L. E. Chipperfield, P. Kinsler, and G. H. C. New, *Phys. Rev. A* **77**, 033806 (2008).
 - [21] L. E. Chipperfield, J. S. Robinson, J. W. G. Tisch, and J. P. Marangos, *Phys. Rev. Lett.* **102**, 063003 (2009).
 - [22] S. Haessler, T. Balčiunas, G. Fan, G. Andriukaitis, A. Pugžlys, A. Baltuška, T. Witting, R. Squibb, A. Zair, J. W. G. Tisch, J. P. Marangos, and L. E. Chipperfield, *Phys. Rev. X* **4**, 021028 (2014).
 - [23] P. Zhang and A. Thomas, *Appl. Phys. Lett.* **106**, 131102 (2015).
 - [24] P. Gibbon, A. Andreev, E. Lefebvre, G. Bonnaud, H. Ruhl, J. Delettrez, and A. Bell, *Phys. Plasmas* **6**, 947 (1999).
 - [25] T. D. Arber, K. Bennett, C. S. Brady, A. Lawrence-Douglas, M. G. Ramsay, N. J. Sircombe, P. Gillies, R. G. Evans, H. Schmitz, A. R. Bell, and C. P. Ridgers, *Plasma Phys. Controlled Fusion* **57**, 113001 (2015).
 - [26] J. Wasserman, K. Lucas, S. Lee, A. Ashton, C. Crowl, and N. Marković, *Rev. Sci. Instrum.* **79**, 073909 (2008).